Efficient Cryogenic Near-Infrared Tm:YLF Laser

CHRIS E. ALESHIRE, CHARLES X. YU, PATRICIA A. REED, AND TSO YEE FAN*

MIT Lincoln Laboratory, 244 Wood Street, Lexington, Massachusetts, 02421, USA
*[*fan@ll.mit.edu](mailto:fan@ll.mit.edu)*

Abstract: Operation of a cw thulium laser emitting at 816 nm has been demonstrated in bulk Tm:YLF with 46% slope efficiency. Prior cw demonstrations of this transition have been limited to ZBLAN fiber hosts and prior lasing in bulk crystalline host material has been limited to quasi-cw operation due to population trapping. Trapping at the $^3F_4$ level was mitigated by co-lasing at 1876 nm. The co-lasing technique should be applicable to room-temperature operation and to power scaling of YLF and other crystal hosts.

OCIS codes: (140.0140) Lasers and laser optics; (140.3580) Lasers, solid-state; (160.3380) Laser materials.

References and links

1. H. Li et al. "Near 1 kW of continuous-wave power from a single high-efficiency diode-laser bar," IEEE Photon. Technol. Lett. **19**(13), 960-962 (2007).
2. X. Liu, M. H. Hu, C. G. Caneau, R. Bhat, and C. Zah, "Thermal management strategies for high power semiconductor pump lasers," IEEE Trans. on Components and Packaging Tech. **29**(2), 268-276 (2006).
3. P. F. Moulton, "Spectroscopic and laser characteristics of Ti:Al$_2$O$_3$," J. Opt. Soc. Am. B **3**, 125-133 (1986).
4. R. K. Huang, B. Chann, L. J. Missaggia, J. P. Donnelly, C. T. Harris, G. W. Turner, A. K. Goyal, T. Y. Fan, and A. Sanchez-Rubio, "High-brightness wavelength beam combined semiconductor laser arrays," IEEE Photon. Technol. Lett. **19**(4), 209-211 (2007).
5. K. J. Creedon, S. M. Redmond, G. M. Smith, L. J. Missaggia, M. K. Connors, J. E. Kansky, T. Y. Fan, G. W. Turner, and A. Sanchez-Rubio, "High efficiency coherent beam combining of semiconductor optical amplifiers," Opt. Lett. **37**(23), 5006-5008 (2012).
6. I. Matsushima, H. Yashiro, and T. Tomie, "10 kHz 40 W Ti:sapphire regenerative ring amplifier," Opt. Lett. **31**(13), 2066–2068 (2006).
7. C. X. Yu, S. J. Augst, S. M. Redmond, K. C. Goldizen, A. Sanchez, D. V. Murphy, and T. Y. Fan, "Coherent combining of a 4 kW, eight-element fiber amplifier array," Opt. Lett. **36**(14), 2686-2688 (2011).
8. Jason K. Brasseur et al. "2.3-kW continuous operation cryogenic Yb:YAG laser," Proc. SPIE **6952**, 69520L (2008).
9. J. Y. Allain, M. Monerie, and H. Poignant, "Tunable CW lasing around 0.82, 1.48, 1.88 and 2.35 µm in thulium-doped fluorozirconate fiber," Electron. Lett. **25**(24), 1660-1662 (1989).
10. J. N. Carter, R. G. Smart, A. C. Tropper, and D. C. Hanna, "Thulium-doped fluorozirconate fibre lasers," J. Non-Crystalline Solids **140**, 10-15 (1992).
11. E. Mejía, L. A. Zenteno, P. Gavrilovic, and A. Goyal, "High-efficiency lasing at 810 nm in single-mode Tm^{3+} doped fluorozirconate fiber pumped at 778 nm," Opt. Eng. **37**(10), 2699-2702 (1998).
12. X. Zhu and N. Peyghambarian, "High-power ZBLAN glass fiber lasers: review and prospect," Adv. in OptoElectron. **2010**, 501956 (2010).
13. B. M. Walsh, N. P. Barnes, and B. Di Bartolo, "Branching ratios, cross sections, and radiative lifetimes of rare earth ions in solids: Application to Tm^{3+} and Ho^{3+} ions in LiYF$_4$," J. Appl. Phys. **83**(5), 2772-2787 (1998).
14. J. A. Caird, L. G. DeShazer, and J. Nella, "Characteristics of room-temperature 2.3-µm laser emission from Tm^{3+} in YAG and YAlO$_3$," IEEE J. Quantum Electron. **11**(11), 874-881 (1975).
15. T. Y. Fan, J. R. Ochoa, and P. A. Reed, "Cryogenic Tm:YAG laser in the near infrared," IEEE J. Quantum Electron. **51**(10), 1700605 (2015).
16. A. Braud, S. Girard, J. L. Doualan, and R. Moncorgé, "Spectroscopy and fluorescence dynamics of (Tm^{3+}, Tb^{3+}) and (Tm^{3+}, Eu^{3+}) doped LiYF$_4$ single crystals for 1.5- µm laser operation," IEEE J. Quantum Electron. **34**(11), 2246-2255 (1998).
17. P. R. Watekar, S. Ju, and W. Han, "800 nm upconversion emission in Yb-sensitized Tm-doped optical fiber," IEEE Photon. Technol. Lett. **18**(15), 1609-1611 (2006).
18. R. Allen, L. Esterowitz, and I. Aggarwal, "An efficient 1.46 µm thulium fiber laser via a cascade process," IEEE J. Quantum Electron. **29**(2), 303-306 (1993).
19. F. Heine, V. Ostroumov, E. Heumann, T. Jensen, G. Huber, and B. H. T. Chai, "CW Yb, Tm:LiYF$_4$ upconversion laser at 650 nm, 800 nm, and 1500 nm," Proc. Adv. Solid-State Lasers **24**, 77-79 (1995).

1. Introduction

The near-infrared (NIR) spectral region around 0.8 μm lacks efficient laser sources with highly scalable diffraction-limited average and peak powers. Two major laser types exist which have found many applications, though neither is well-suited for both peak- and average-power scaling. AlGaAs diode systems, while relatively simple in design and highly efficient, have low energy storage ability due to short recombination times, limiting peak power and requiring the use of low-brightness bar and stack configurations for power scaling [1]. Additionally, thermal handling requirements dictate low pulse energies and repetition rate in diode systems [2]. Titanium-doped Sapphire (Ti:S) systems [3] can provide excellent beam quality, high pulse energies, and very high peak power due to the material's large emission bandwidth, but this comes at the cost of significant complexity as the optical properties of the material itself result in inefficient systems. Despite several decades of research and development, diffraction-limited average powers of GaAs-based diodes and Ti:S lasers have reached only tens of watts [4-6]. In contrast, 1 μm diode-pumped solid state lasers (DPSSLs), fiber lasers, and beam-combined systems thereof commonly achieve powers >1 kW with near-ideal beam quality [7, 8].

A third source of 0.8 μm NIR laser emission which has potential for scaling to very high powers is in Tm^{3+}-doped materials on the $^3H_4 - {}^3H_6$ transition. This transition can be pumped with low quantum defect by AlGaAs diode sources emitting at $0.78 - 0.8$ μm. These systems have the potential to scale to high peak and average powers with relatively simple designs. Highly efficient lasing has been demonstrated in Tm^{3+}-doped fluorozirconate (ZBLAN) fibers [9-11] but these systems are not promising candidates for scaling power or energy due to the difficulty in manufacturing high purity materials [12], the poor thermal and mechanical properties of ZBLAN, and the fiber geometry. There has been little further development of these materials for NIR Tm^{3+} lasers in the last decade. Bulk crystal hosts are more attractive for power scaling because of their higher thermal conductivity and larger apertures than ZBLAN fiber. In crystal hosts $Y_3Al_5O_{12}$ (YAG) and $YLiF_4$ (YLF), the NIR transition in Tm^{3+} is similar to the 1 μm laser transition in Yb^{3+}, with comparable emission bandwidth and a 1-2 ms upper state lifetime suitable for high-power operation [13,14].

2. Thulium laser key physics

Lasers based on Tm-doped media are well-established as infrared sources emitting wavelengths around 1.9 μm. Fig. 1 depicts a simplified diagram of the energy levels associated with this transition and the NIR transition. Concentration quenching in highly doped media enables emission of two fluorescence photons for each pump photon (the "2 for 1" effect), doubling the effective quantum efficiency in these systems. Radiative decay from $^3H_4$ to $^3F_4$ can also occur with emission wavelengths of 1.5 μm or 2.3 μm. Laser operation on these transitions has been achieved, but must contend with the long lifetime of the $^3F_4$ state which serves as a lower laser level for these transitions. Although the NIR transition of interest here does not directly decay to $^3F_4$, alternate decay paths such as multiphonon and cross relaxation must be carefully considered for lasers operating on this transition as each presents a potential source of loss to the desired NIR laser. Specifically, as the radiative lifetimes of $^3H_4$ and $^3F_4$ are of order 1 ms and 10 ms, respectively, continuous pumping with significant rate of branching to $^3F_4$ results in accumulation and trapping of the population at this level, reducing pump absorption.

Recently, quasi-cw NIR lasing of diode-pumped Tm:YAG at liquid nitrogen temperature was demonstrated with 36% slope efficiency [15]. The laser's output duration was limited by population trapping at the $^3F_4$ level and quasi-CW pumping was necessary to allow the trapped population to spontaneously decay to the ground state. For durations greater than several tens of milliseconds, the laser's output was ultimately extinguished through this bleaching mechanism. This demonstration confirmed that population trapping is a key physics issue in Tm-doped bulk crystal lasers operating on this transition and that cw operation

requires mitigation of this trapping. Potential mitigation strategies may include selection of the crystal host to minimize non-radiative decay rates, co-doping to quench the $^3F_4$ lifetime [16], upconversion schemes to pump out of $^3F_4$ [17], or quenching by stimulated emission on the $^3F_4 - {}^3H_6$ transition [18]. There has been a report of operation on the NIR transition in a bulk crystal, Tm:YLF, by upconversion pumping, but no data were reported [19]. Upconversion pumping is unattractive as it is less efficient than single photon schemes.
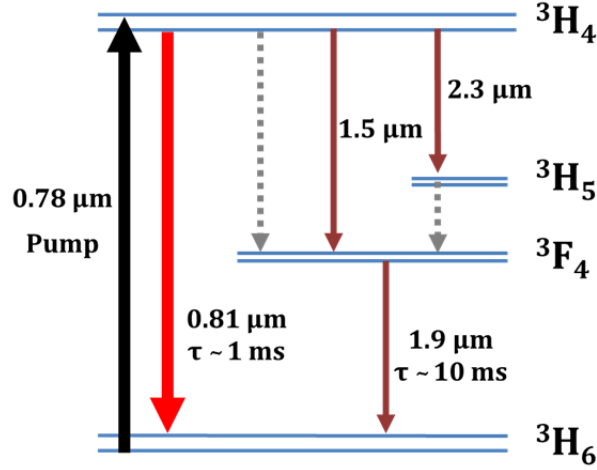

Fig. 1 Energy level diagram of Tm^{3+} showing the numerous transitions stemming from the $^3H_4$ level and order of magnitude lifetimes in crystal hosts. Dotted lines indicate non-radiative transitions.

The effect of population trapping can be modelled with a rate equation analysis [15]. An analysis for trapping in Tm:YAG reveals a significantly higher population trapped in $^3F_4$ than in the upper laser level $^3H_4$. For example, in 1%-doped Tm:YAG, this analysis predicts the steady-state population in $^3F_4$ is 26 times that in $^3H_4$ if no mitigation is applied. The same analysis is extensible to other crystal hosts with substitution of the appropriate rate constants. Concentration quenching and multi-phonon relaxation are the two dominant non-radiative decay mechanisms. Concentration quenching can be minimized by keeping dopant concentrations to 1% or less [14], while the multi-phonon lifetime is largely determined by the host material. Due to their lower characteristic phonon energies, fluoride crystals (YLF, CaF_2, etc.) in general have lower non-radiative decay rates than oxide crystals (YAG, YVO_4, $YAlO_3$, etc.), and are likely candidates for improved efficiency and cw operation. Even so, residual trapping due to concentration quenching and alternative radiative decay paths can require additional mitigation strategies.

3. Laser experiments and results

As mentioned above, fluoride crystals are more favorable hosts for operation at the NIR transition in Tm^{3+}. The measured absorption and emission spectra of Tm^{3+}:YLF at 300 K and 80 K are graphed in Fig. 2. The absorption features are directly accessible with AlGaAs diode systems. The effective stimulated emission cross sections were calculated from the fluorescence spectra, a radiative lifetime of 2 ms [16], and a spontaneous decay branching ratio from $^3H_4 - {}^3H_6$ of 0.9 [13]. The room temperature absorption and effective emission cross sections are in reasonable agreement with a previous report [13].
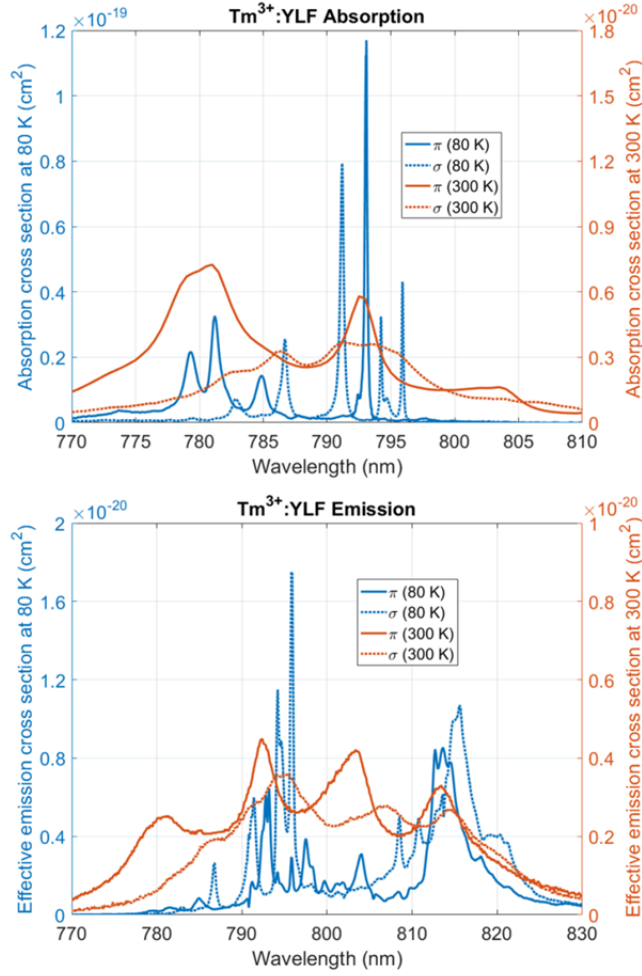
Fig 2. Absorption (top) and emission (bottom) spectra of Tm^{3+}:YLF at 80 K and 300 K. The laser was pumped at 781.5 nm and operated at 816 nm.

Although Tm:YLF has lower nonradiative decay rate than Tm:YAG, residual population trapping still affects laser performance. Co-lasing on the 1.9 μm transition can be used to continuously quench the trapped population by stimulated emission. As this transition is not directly accessed from the $^3H_4$ level, co-lasing does not compete with the NIR transition. Also, from the rate equation analysis [15], the $^3F_4$ population is proportional to the $^3H_4$ population, and consequently, the 1.9 μm output power is expected to remain constant with increasing pump power above laser threshold for both transitions. To validate these predicted dynamics, a proof-of-principle dual-wavelength laser was constructed using a 0.5%-doped Tm:YLF crystal fabricated to ~15 mm length and cryogenically cooled to liquid nitrogen temperature. Cryogenic cooling was used to reduce the Tm^{3+} population in the lower laser level and enhance absorption features, reducing threshold and enabling operation with lower-power pump sources.

The laser was constructed as an end-pumped hemispherical cavity, with a flat dichroic and 250 mm radius-of-curvature output coupler. The dichroic was anti-reflection coated at the pump wavelength (781.5 nm) and high-reflection coated at the NIR and infrared Tm^{3+} emission bands. The output coupler was 3% transmissive at both lasing wavelengths and 97% reflective at the pump wavelength. At 80 K the single-pass pump absorption was 47%, resulting in double-pass absorption of ~70% in the cavity. The crystal was pumped using a

Ti:S laser with output wavelength and polarization tuned to maximize absorption in the crystal. The pump beam was focused to a diameter of 160 μm in the crystal.

The laser performance is graphed in Fig. 3 for cw pumping at liquid nitrogen temperature. The output wavelengths were separated using a polished silicon window. The operating wavelengths were 816 nm and 1876 nm, with respective slope efficiencies 46% and 4% versus incident pump power. The fitted NIR threshold was 246 mW, and the maximum NIR output was 339 mW, limited by the 1 W TiS pump laser. The NIR output polarization was orthogonal to the pump polarization, as expected based on Fig. 3 (π pump orientation and σ emission orientation). The low-efficiency 1.9 μm signal agrees well with predictions based on rate analysis. A plane-wave analysis predicts the slope efficiency for the 1.9 μm output should be 0, and the fact that the observed slope efficiency is non-zero, but low, can be attributed to the Gaussian beam nature of the pump and laser outputs.
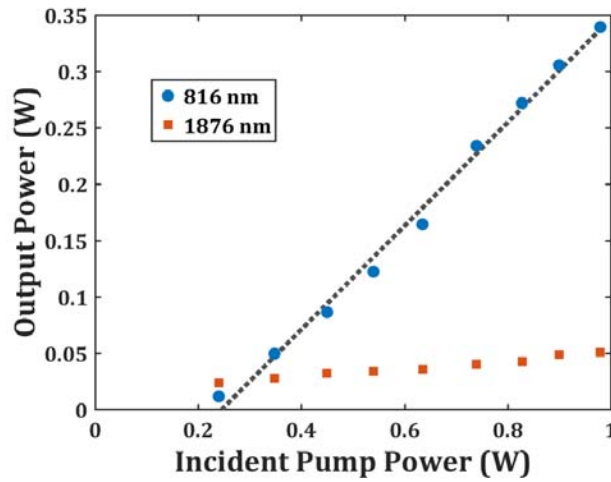

Fig. 3. Output power as a function of incident pump power for the dual wavelength Tm^{3+}:YLF laser system.

To investigate operation at higher temperatures, the laser was run at full pump power (1 W) while monitoring temperature and output signal as the liquid nitrogen evaporated. Lasing was achieved for temperatures up to 200 K, however this does not represent a physical limit to the laser operation. As mentioned previously, cryogenic operation lowers threshold by depopulating the lower laser level and increasing the absorption and stimulated emission cross sections. It is expected that with the use of higher-power pump sources (AlGaAs diode arrays, for instance), the laser can be run at or near room temperature, albeit with higher threshold power than in this proof-of-principle demonstration.

4. Summary

Efficient cw laser operation of the NIR transition in Tm^{3+}:YLF at 816 nm has been demonstrated. This is an improvement over a previous demonstration in Tm:YAG which required quasi-cw pumping to mitigate population trapping at the $^3F_4$ manifold. Trapping mitigation in these experiments was mitigated by cryogenic cooling, use of a YLF crystal host to reduce nonradiative decay rates and the use of a dual-wavelength resonator to continuously quench the trapped population by stimulated emission on the $^3F_4 - {}^3H_6$ transition. Bulk crystal systems have a clearer pathway to scaling and optimization than do previously demonstrated non-crystal hosts. The ability to operate crystal lasers continuously on this transition expands their potential for use as high peak and average power sources.

Acknowledgements